

# Aggregation and Adsorption at the Air-Water Interface of Bacteriophage $\phi$ X174 Single-Stranded DNA

C. Douarche,<sup>\*†‡</sup> J.-L. Sikorav,<sup>§</sup> and A. Goldar<sup>†</sup>

<sup>\*</sup>Physique de la Matière Condensée, Ecole Polytechnique, Centre National de la Recherche Scientifique, Palaiseau, France;

<sup>†</sup>Service de Biologie Intégrative et de Génétique Moléculaire, Commissariat à l'Énergie Atomique, Gif-sur-Yvette, France;

<sup>‡</sup>Institut de Recherche Interdisciplinaire, Cité Scientifique, Villeneuve d'Ascq, France; and <sup>§</sup>Service de Physique Théorique, Commissariat à l'Énergie Atomique, Gif-sur-Yvette, France

**ABSTRACT** We study the phase behavior of phage  $\phi$ X174 single-stranded DNA in very dilute solutions in the presence of monovalent and multivalent salts, in both water ( $H_2O$ ) and heavy water ( $D_2O$ ). DNA solubility depends on the nature of the salts, their concentrations, and the nature of the solvent. The appearance of attractive interactions between the monomers of the DNA chains in the bulk of the solution is correlated with an adsorption of the chains at the air-water interface. We characterize this correlation in two types of aggregation processes: the condensation of DNA induced by the trivalent cation spermidine and its salting out in the presence of high concentrations (molar and above) of monovalent (sodium) cations, both in water and in heavy water. The overall solubility of single-stranded DNA is decreased in  $D_2O$  compared to  $H_2O$ , pointing to a role of DNA hydration in addition to electrostatic factors in the observed phase separations. DNA adsorption involves attractive van der Waals forces, and these forces are also operating in the bulk aggregation process.

## INTRODUCTION

The physical chemistry and biochemistry of DNA can be studied using two lines of research. The first one focuses on the behavior of nucleic acids in the bulk of homogeneous aqueous solutions (1–5). In this approach, phase separations such as aggregation, precipitation, or adsorption are carefully avoided; from a physical point of view, the interactions between the monomers of double-stranded DNA chains remain repulsive. This approach has been traditionally the main line of research followed by scientists in the field. In parallel, over the last decades, there has been a growing interest for the study of DNA in heterogeneous systems, in particular systems where DNA either undergoes aggregation and precipitation or interacts with surfaces.

The motivations for this second approach come from both fundamental and applied considerations. A major issue is that of DNA condensation. Long DNA molecules exist in vivo in condensed states, and it is an important goal of molecular biology to understand the consequences of these dense conformations on the structure and on the function of the genetic material. In *E. coli*, for instance, the nucleoid consists of condensed chromosomal DNA, which is phase-separated from the surrounding cytoplasmic proteins (6). Dense states of DNA can be obtained in vitro in simple systems using various condensing agents such as multivalent cations or polyethylene glycol plus the monovalent salt sodium chloride. Physically, the condensing agents act by introducing interactions that are effectively attractive be-

tween the monomers of the DNA chains, leading to the collapse of long chains in very dilute solutions and also to the aggregation and precipitation of the chains in less dilute systems (see (5) and (7) for reviews). This corresponds to what is called poor solvent conditions in polymer physics. The study of the dense states of DNA found in vivo using in vitro systems requires, therefore, an understanding of its behavior in heterogeneous systems (where phase separations due to aggregation take place), in contrast with the traditional approach discussed above.

A second issue is concerned with the interactions between DNA and interfaces. In a general manner, interfaces have a key role in biological systems (8); biological membranes, in particular, play an essential structural and functional role in the cells. The importance of the interactions of DNA with membranes can be seen in the process of genetic transformation: DNA molecules have to cross membranes when they enter cells. As stated by Kahn and Smith, genetic transformation is therefore (in part) a problem of membrane biology (9). DNA-interface interactions occur also in many other physiological situations, as described below.

DNA in vivo is not naked but is usually associated with proteins and enzymes. This association can be viewed as an interaction with the surface of the associated proteins; this view is extremely useful in the study of DNA topology (10,11). DNA located at interfaces in vitro constitutes a simple model system, which can contribute to our understanding of the more complex nucleic acid-protein interactions.

DNA in vivo does not have the space available in the bulk of a dilute aqueous solution. Quite on the contrary, both its structure and its motion are highly constrained due to interactions with structural elements such as the inner face of a viral capsid, the outer or inner face of a bacterial membrane,

Submitted March 2, 2007, and accepted for publication July 23, 2007.

Address reprint requests to Jean-Louis Sikorav, Service de Physique Théorique, CEA/Saclay, 91191 Gif-sur-Yvette Cedex, France. E-mail: jean-louis.sikorav@cea.fr.

Editor: Jonathan B. Chaires.

© 2008 by the Biophysical Society  
0006-3495/08/01/134/13 \$2.00

doi: 10.1529/biophysj.107.107771

the inner face of a nuclear envelope (through the nuclear lamina and the nuclear pores), and possibly the nuclear matrix in eukaryotic cells (12). Again, the study of the interfacial properties of DNA in simple in vitro systems is expected to shed light on these more complex interactions.

A third reason motivating the study of nucleic acids in heterogeneous systems comes from the observation that such systems can in fact be more efficient than the conventional homogeneous systems (13). Indeed, the efficiency of DNA renaturation (7,13,14) and cyclization (15) is much higher in systems where the DNA chains undergo a phase separation coupled with the ongoing reaction. In these reactions, two types of phase separations are considered: 1), a bulk phase separation due to the presence of DNA condensing agents, leading to an aggregation process concomitant with renaturation (7,14) or cyclization (15); and 2) a transfer of the DNA chains from the bulk of an aqueous solution to a water-phenol interface concomitant with an interfacial renaturation (13).

These findings highlight the limitations of the conventional, homogeneous approach of DNA physical chemistry and biochemistry. The study of heterogeneous systems also leads to a better understanding of the behavior of DNA in vivo. For example, the high rates of cyclization of  $\lambda$  DNA observed in the presence of condensing agents are fast enough to account for the cyclization of the chain observed after it is injected into its bacterial host; In contrast, the rates measured in homogeneous systems are too slow to account for this process (15).

Besides its fundamental interest, the study of nucleic acids in heterogeneous systems is also of great importance from an applied point of view. For example, a number of separation techniques of nucleic acids rely on the use of heterogeneous systems (liquid-liquid extraction, precipitation, chromatographic techniques). In addition, many hybridization technologies (Southern or Northern blots, hybridization on chips) involve nucleic acids immobilized on surfaces. Nanotechnologies have a growing impact on interfacial hybridization techniques. In microfluidics, for instance, the surface/volume ratio is large, and this requires an understanding of the interaction between nucleic acids and substrate. For yet another example, the visualization of nucleic acids by microscopy relies in an essential manner on the interaction of nucleic acids with surfaces, either in the standard techniques of electron microscopy (5) or in the more recent approaches using scanning tunneling or atomic force microscopy (AFM) (16,17). AFM, in particular, is used to investigate DNA condensation (18,19), raising the issue of the link between bulk effects (aggregation) and surface effects (adsorption).

Therefore, a better understanding of the behavior of nucleic acids in heterogeneous systems could contribute to understanding and improving these new techniques.

In this work, we investigate the phase separations occurring in very dilute aqueous solutions of single-stranded DNA in the presence of mono- and multivalent cations. Two previous works prompted us to undertake this investigation:

The first one is a careful study by Frommer and Miller (20) of the adsorption of DNA at the air-water interface. These authors used tritiated DNA to measure directly the adsorption of *E. coli* DNA at the air-water interface. They worked with both native (double-stranded) and denatured (mostly single-stranded) DNA. They observed an adsorption of double-stranded DNA at the air-water interface, which (at a constant DNA concentration of  $26 \mu\text{g ml}^{-1}$ ) increased with the concentration of NaCl between 1 mM and 1 M. The amount of double-stranded DNA adsorbed at 1 M NaCl increased with bulk DNA concentration, reaching a plateau above  $75 \mu\text{g ml}^{-1}$  of  $\sim 1.8 \text{ mg m}^{-2}$  which corresponds to an area of  $\sim 0.31 \text{ nm}^2$  per nucleotide, the value expected for a monolayer of densely packed DNA double helices. Fibers could easily be drawn from the adsorbed DNA layer. Surprisingly, in this work, the adsorption of the DNA chains did not lead to a change in the surface tension or the surface potential. Denatured DNA (immersed in boiling water for 10–15 min and then cooled in a water-ice mixture) was also studied and found to adsorb at 1 M NaCl, albeit in a less efficient manner.

In a later work, Eickbush and Moudrianakis (21) studied the adsorption at the air-water interface of double-stranded DNA molecules (10-kilobase-long DNA chains of the phage PM2) in the presence of a variety of chemical compounds. The adsorption was assayed by touching the solution surface with an electron microscope grid and by counting the number of DNA chains found on the grid. These authors used more dilute DNA solutions (with typical concentrations in the range of  $0.1\text{--}0.5 \mu\text{g ml}^{-1}$ ). They also observed an adsorption in the presence of monovalent salts, which increased with the salt concentration (between 10 mM to 1 M), in qualitative agreement with the observations of Frommer and Miller (20). In addition, they studied the effect of a trivalent cation, spermidine, a natural polyamine that promotes the condensation of nucleic acids, and made two observations: 1), spermidine also led to an adsorption of the DNA at the air-water interface that increased with spermidine concentration; and 2), the concentration range over which this adsorption could be observed was very narrow, since a bulk precipitation of the chains occurred soon after the onset of the adsorption. Thus, it appears that in this latter case, the adsorption process could take place at the same time as a precipitation. This latter finding is puzzling, since it raises the possibility that previous studies devoted to the condensation of nucleic acids could have overlooked a concomitant adsorption at the air-water interface.

To investigate this issue, we performed a series of experiments to probe both DNA aggregation and precipitation and DNA adsorption at the air-water interface. We report here the results obtained for single-stranded DNA molecules (prepared from the bacteriophage  $\phi\text{X174}$  (22)). We decided to work with very dilute solutions ( $5\text{--}15 \text{ ng ml}^{-1}$ ) to favor the detection of surface effects over bulk effects. We also chose to use two types of salts to promote

DNA aggregation: sodium chloride and the trivalent cation spermidine. Sodium chloride is known to induce the aggregation of single-stranded nucleic acids at high concentrations (typically 1 mol and above). This type of aggregation is called a salting out. The best example of it is the aggregation of polyriboadenylic acid (polyA) by sodium chloride studied by Eisenberg and Felsenfeld (23). Multivalent cations also induce an aggregation, to which we will specifically refer from now on as a condensation. (Nucleic acid condensation is a generic term for collapse and aggregation, which includes condensation by multivalent cations and by other agents such as polyethylene glycol plus sodium chloride. The salting out of nucleic acids by monovalent cations is, in this generic sense, a particular type of condensation. For clarity, however, we restrict the use of the term condensation in the rest of the text to specifically describe the action of multivalent cations; we refer to the action of monovalent cations as “salting out”.) The corresponding phase diagrams for DNA condensation, both for double-stranded (24,25) and single-stranded DNA (14,26,27), have been studied in detail. These phase diagrams reflect the polyelectrolyte behavior of DNA, irrespective of its secondary structure. Indeed, similar phase diagrams are observed not only with double- and single-stranded DNA and with nucleosomes (27), but also with synthetic polyelectrolytes such as polystyrene sulfonate (28). The mechanisms of DNA aggregation (whether salting out or condensation) are complex (see (5) for a detailed review in the case of DNA condensation). Both in DNA salting out and DNA condensation, electrostatic interactions play an essential role: the addition of salts decreases the electrostatic repulsion between chain monomers. However, it is also well known that nonelectrostatic factors play a role both in salting out and condensation: The very high salt concentrations required for the salting out leads to a decrease in the water activity (29). DNA hydration is also implied in the condensation process (30,31). Electrostatic and hydration forces both have a positive entropic contribution, but are difficult to distinguish in an aqueous environment (32). To further explore the relative contributions of electrostatic and hydration factors in DNA aggregation and adsorption, in this work we obtained experimental results both in water (H<sub>2</sub>O) and heavy water (D<sub>2</sub>O).

## MATERIAL AND METHODS

### Chemicals

Deionized water obtained from a Milli-Q filtration system (Millipore, Molsheim, France) was used in all studies. Spermidine 3HCl (molecular biology grade), sodium chloride and deuterium oxide (D<sub>2</sub>O) was obtained from Sigma-Aldrich (Saint-Quentin Fallavier, France).

Circular single-stranded  $\phi$ X174 virion DNA (molecular mass  $1.7 \times 10^6$  Da, 5386 bases) was purchased from New England Biolabs (Ozyme, Saint-Quentin, France). The circular DNA was linearized as follows: an 18-base-long oligodeoxynucleotide (5'-TAGTGGAGGCCTCCAGCA-3') was purchased from MWG Biotech (Ebersberg, Germany). This fragment contains the complementary sequence of nucleotides 4481–4497 of  $\phi$ X174 virion

DNA, which includes the recognition site of the restriction endonuclease enzyme StuI (at nucleotide 4486). The oligonucleotide was annealed with the circular single-stranded  $\phi$ X174 virion DNA. The annealing process was carried out in a  $1 \times$  NEB2 buffer (New England Biolabs) using a molar ratio of 1000:1 for the 18-base-long fragment over the  $\phi$ X174 virion DNA chains (for a typical reaction, we use 40  $\mu$ g of  $\phi$ X174 virion). The solution was heated to 98°C for 3 min to remove the secondary structures of  $\phi$ X174 virion DNA. The solution was then left to cool down at room temperature overnight. We added 80 units of the restriction enzyme StuI to the cooled solution. After 2 h of incubation at 37°C, the digested DNA was analyzed by agarose gel electrophoresis, which showed that the circular DNA present initially in the solution had been fully linearized.

### Plasticware

The radioactive detection experiments described in this work were all performed at extremely low concentrations of single-stranded DNA (with chain concentrations in the picomolar range). Low DNA concentrations coupled with high salt concentrations can lead to a significant adsorption on the walls of the polypropylene centrifuge tubes used (either Eppendorf or Falcon) if no specific precautions are taken. To prevent this effect, all experiments were carried out using tubes coated with a methyl brush, obtained as follows: the tubes were filled with a solution of 2% dimethyldichlorosilane in (1,1,1)-trichloroethane. After ~6 h of incubation, the silane solution was removed and the tubes were thoroughly rinsed with a TE buffer (10 mM Tris-HCl, pH 7.5, 1 mM EDTA).

### DNA labeling

The 5'-end of the phosphate group of the linearized  $\phi$ X174 virion DNA was removed using a calf alkaline phosphatase enzyme purchased from New England Biolabs. After 1 h of reaction at 37°C, the solution was purified using a Sigma PCR Clean Kit. The product of the reaction was 5'-end labeled with T4 polynucleotide kinase (New England Biolabs) using <sup>32</sup>P-ATP (>6000 Ci mmol<sup>-1</sup>, GE Healthcare Life Sciences, Orsay, France). The labeled single-stranded DNA was separated from the unincorporated <sup>32</sup>P-ATP using a Sigma GenElute PCR Clean-Up Kit and eluted in a TE buffer (10 mM Tris-HCl, pH 7.5, 1 mM EDTA). The amount of unincorporated <sup>32</sup>P-ATP still present in the solution of labeled single-stranded DNA after purification was determined by an autoradiogram of a sample submitted to separation by agarose gel electrophoresis. The unincorporated <sup>32</sup>P-ATP accounted for 1% or less of the total radioactivity present in the solution of labeled single-stranded DNA. To avoid a contamination of the DNA samples with surface active agents, none of the protocols used above involved surfactants.

### Studies of the solubility of $\phi$ X174 virion DNA by sedimentation

These experiments were performed using 1.5-ml Eppendorf tubes as follows. The labeled single-stranded DNA (200  $\mu$ l containing the labeled single-stranded DNA at a concentration of 4.2 pg/ $\mu$ l in a TE buffer (deuterated or hydrogenated, with various concentrations of NaCl and/or spermidine)) was placed in an Eppendorf tube. After vortexing, the tube was left for at least 12 h to equilibrate at room temperature. The tubes were then centrifuged at  $15,000 \times g$  for 5 min. After centrifugation, half of the solution was removed and collected in a separate tube. Thin cones were used to avoid extensive contact with the air-water interface during the pipetting. The amount of radioactivity was measured both in the collected 100  $\mu$ l (count<sub>solution</sub>) and the remaining 100  $\mu$ l (count<sub>remaining</sub>) solutions using a Beckmann scintillation counter in the Cerenkov mode. The fraction of soluble DNA remaining in the bulk of the solution after centrifugation was determined using the formula

$$\text{soluble DNA} = 2 \times \frac{\text{count}_{\text{solution}}}{\text{count}_{\text{solution}} + \text{count}_{\text{remaining}}}. \quad (1)$$

The change of regimes of solubility with salt concentration was obtained by drawing tangents to the experimental curves and determining the intersections of these tangents (see Fig. 2 *a*).

### Studies of the solubility of $\phi$ X174 virion DNA combining autoradiography and sedimentation

These experiments were performed using the much larger, 15-ml conical Falcon centrifuge tubes as follows: 10 ml of a TE buffer solution (deuterated or hydrogenated, with various concentrations of NaCl and/or spermidine) containing the radioactively labeled  $\phi$ X174 virion DNA at a concentration of  $15.3 \text{ pg } \mu\text{l}^{-1}$  was placed in a Falcon tube. After vortexing, the tube was left to stand for at least 12 h. The tubes were first exposed for 12–16 h to a storage phosphor autoradiography plate (Molecular Dynamics, Sunnyvale, CA), which was scanned using a Phosphor Imager (Molecular Dynamics). The tubes were then centrifuged at  $4500 \times g$  for 20 min. After centrifugation, the tubes were again exposed for at least 12 h to an erased autoradiography plate. This exposed plate was then scanned as above. The quantification of the number of counts as a function of the height of the tube was measured using the ImageQuant software (GE Healthcare, Waukesha, WI). After background subtraction and normalization of the area under the curve (which corresponds to the total amount of radioactivity in the tube), the fraction of counts was plotted as a function of the height of the tube. We measured not an absolute number of counts but a relative value.

## RESULTS

### Sedimentation studies of DNA solubility

In the first series of experiments, we measured the amount of DNA remaining in the supernatant of centrifuged Eppendorf tubes for various concentrations of  $\text{Na}^+$  and  $\text{Spd}^{3+}$  (spermidine  $3^+$ ). We refer to this material as “soluble DNA”. The material depleted from the supernatant can either be incorporated in a precipitated pellet or else adsorbed at the air-water interface. The distinction between these two possibilities, as well as a better description of the “soluble DNA”, will be made later in discussing the autoradiography studies.

#### Salting out in the presence of NaCl

Fig. 1 shows the effect of increasing amounts of NaCl on the solubility of  $\phi$ X174 DNA in  $\text{H}_2\text{O}$  and in  $\text{D}_2\text{O}$ . At high salt concentration, the solubility is reduced. This is a salting out, and we label the value of the concentration at which the onset of reduced solubility takes place  $C_S$ .  $C_S = 1.5 \text{ M}$  for  $\text{D}_2\text{O}$  and  $2.5 \text{ M}$  for  $\text{H}_2\text{O}$ .  $\phi$ X174 DNA is therefore less soluble in  $\text{D}_2\text{O}$  than in  $\text{H}_2\text{O}$ .

#### Condensation in the presence of $\text{Spd}^{3+}$ and NaCl

Fig. 2 *a* shows the change in solubility of  $\phi$ X174 DNA as a function of  $\text{Spd}^{3+}$  concentration at a fixed NaCl concentration ( $10^{-2} \text{ M}$  for both  $\text{D}_2\text{O}$  and  $\text{H}_2\text{O}$ ). In both cases, the DNA is fully soluble at low  $\text{Spd}^{3+}$  concentration. The solubility starts to decrease at a concentration  $C_1$  and then reaches a plateau of low solubility at a concentration  $C_2$ . This plateau ends at a concentration  $C_3$ . For  $\text{H}_2\text{O}$  only, a further increase in  $\text{Spd}^{3+}$  concentration leads to a full resolubilization of the

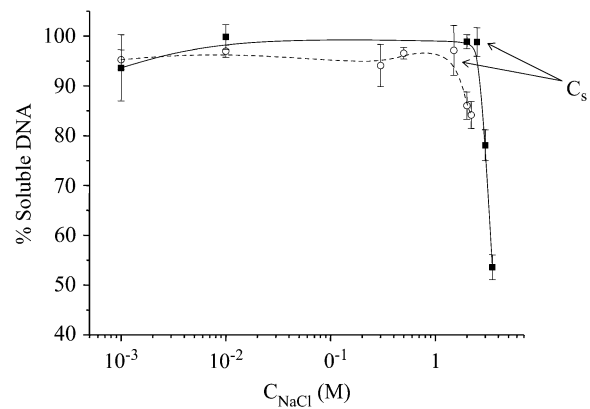


FIGURE 1 Percentage of soluble single-stranded DNA as a function of NaCl concentration in  $\text{D}_2\text{O}$  (open circles) and  $\text{H}_2\text{O}$  (solid squares). The concentrations at which the solubility starts to decrease ( $C_S$ ) are indicated by arrows (1.5 M NaCl in  $\text{D}_2\text{O}$  and 2.5 M NaCl in  $\text{H}_2\text{O}$ ). The solid and dashed black lines are guides for the eyes.

DNA at a concentration  $C_4$ . Due to lower spermidine solubility in  $\text{D}_2\text{O}$ , it is not possible to increase the concentration to this value in  $\text{D}_2\text{O}$ . A comparison of the results obtained in  $\text{D}_2\text{O}$  and  $\text{H}_2\text{O}$  shows that:

1. The concentrations of the onset in decreased solubility,  $C_1$ , and the beginning of the plateau of minimal solubility,  $C_2$ , are lower in  $\text{D}_2\text{O}$  than in  $\text{H}_2\text{O}$ , with an  $\sim 10$ -fold difference between the two solvents.
2. The concentration  $C_3$ , at which the plateau of minimal solubility ends, is similar for the two solvents.
3. The value for the plateau of minimal solubility is lower in  $\text{D}_2\text{O}$  ( $\sim 5\%$ ) than in  $\text{H}_2\text{O}$  ( $\sim 20\%$ ).

We conclude, in this experiment, that  $\phi$ X174 DNA is less soluble in  $\text{D}_2\text{O}$  than in  $\text{H}_2\text{O}$ .

1. Less  $\text{Spd}^{3+}$  is needed to decrease the solubility in  $\text{D}_2\text{O}$  than in  $\text{H}_2\text{O}$ .
2. The plateau of minimal solubility is broader in  $\text{D}_2\text{O}$  and has a lower value than in  $\text{H}_2\text{O}$ .

However, the concentration  $C_3$  is independent of the solvent.

Fig. 2 *b* shows the change in solubility of  $\phi$ X174 DNA as a function of NaCl concentration at a fixed  $\text{Spd}^{3+}$  concentration (10 mM), both for  $\text{D}_2\text{O}$  and  $\text{H}_2\text{O}$ . In both cases, the DNA is in the region of minimal solubility at low NaCl concentration. This first region ends at a concentration  $C_A$  above which the solubility increases. The second region ends at a concentration  $C_B$  where the DNA is again fully soluble. Finally, the solubility starts to decrease again at 1.5 M NaCl for  $\text{D}_2\text{O}$  and 2.5 M NaCl for  $\text{H}_2\text{O}$ . These two concentrations are identical to the  $C_S$  concentrations measured for salting out in the absence of  $\text{Spd}^{3+}$ , discussed above, and are also denoted  $C_S$ . The values measured for the plateau of minimal

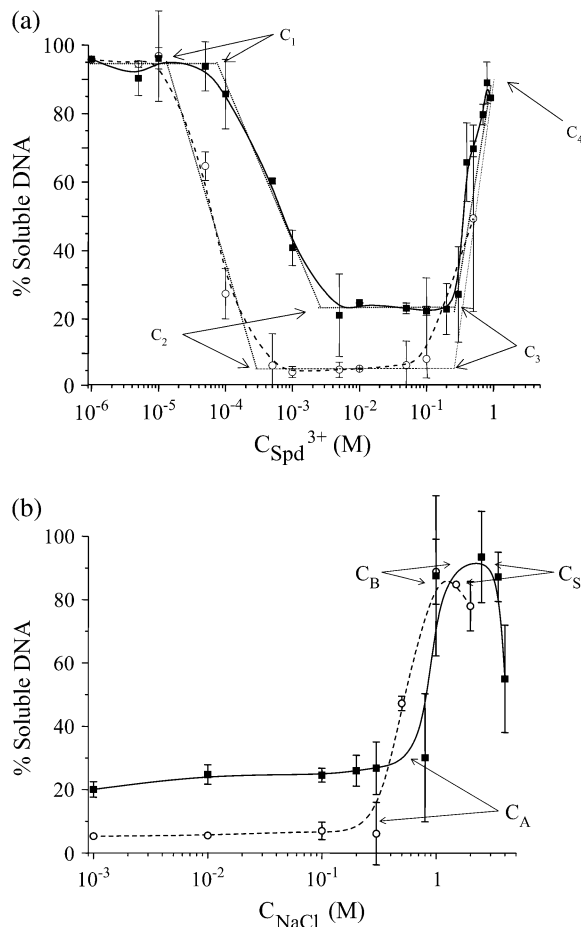


FIGURE 2 (a) Percentage of soluble single-stranded DNA as a function of  $\text{Spd}^{3+}$  concentration at  $10^{-2}$  M NaCl in  $\text{D}_2\text{O}$  (open circles) and  $\text{H}_2\text{O}$  (solid squares). The  $\text{Spd}^{3+}$  concentrations  $C_1$ ,  $C_2$ ,  $C_3$ , and  $C_4$  correspond to the onset of the solubility decrease, the onset of the minimum of solubility, the end of the minimum, and the end of the solubility decrease, respectively, and are indicated by arrows. The concentrations  $C_1$ ,  $C_2$ , and  $C_3$  are obtained by drawing tangents (thin dotted lines) to the experimental curves and determining the intersections of these tangents. The solid and dashed black lines are guides for the eyes. (b) Percentage of soluble single-stranded DNA as a function of NaCl concentration at  $10^{-2}$  M  $\text{Spd}^{3+}$  in  $\text{D}_2\text{O}$  (open circles) and  $\text{H}_2\text{O}$  (solid squares). The concentrations  $C_A$ ,  $C_B$ , and  $C_S$  correspond to the end of the minimum of solubility, the end of the solubility decrease, and the reappearance of the solubility decrease, respectively, and are indicated by arrows. The solid and dashed black lines are guides for the eyes.

solubility (0–10% for  $\text{D}_2\text{O}$ , 10–30% for  $\text{H}_2\text{O}$ ) are those found in the experiments described in Fig. 2 a. At 10 mM  $\text{Spd}^{3+}$ , a greater amount of NaCl is required to resolubilize DNA in  $\text{H}_2\text{O}$  than in  $\text{D}_2\text{O}$ .

### General phase diagrams

We repeated the experiments described above for various concentrations of NaCl and  $\text{Spd}^{3+}$  and used the combined results to plot the solubility behavior of  $\phi\text{X174}$  in the plane of coordinates ( $[\text{NaCl}]$ ,  $[\text{Spd}^{3+}]$ ), for both  $\text{H}_2\text{O}$  (Fig. 3) and  $\text{D}_2\text{O}$  (Fig. 4).

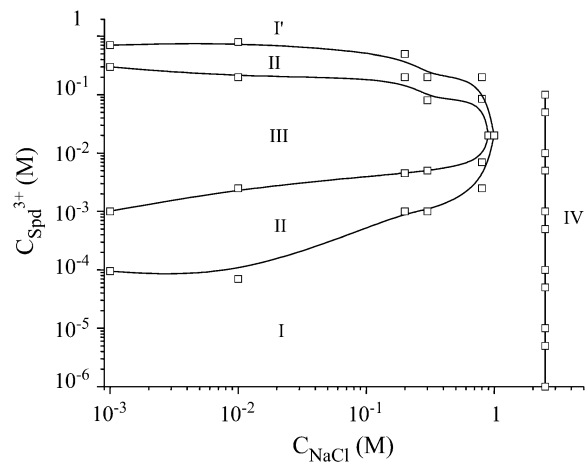


FIGURE 3 Plot of the concentrations  $C_1$ ,  $C_2$ ,  $C_3$ ,  $C_4$ ,  $C_A$ ,  $C_B$ , and  $C_S$  in the plane of coordinates ( $[\text{NaCl}]$ ,  $[\text{Spd}^{3+}]$ ) in  $\text{H}_2\text{O}$ . Five distinct regions are observed. The regions I, II, III, and I' are delimited by solid lines, which are guides for the eyes. Region I, the first soluble phase; Region II, a region where the solubility of DNA in the presence of  $\text{Spd}^{3+}$  varies; Region III, a region where the solubility of DNA in the presence of  $\text{Spd}^{3+}$  is constant and minimal; Region IV, a region above which the DNA is salted out by NaCl, separated from region I by a solid vertical line at 2.5 M NaCl; and Region I', the second soluble phase.

Fig. 3 shows the phase diagram obtained for  $\text{H}_2\text{O}$ .

Broadly speaking, there are two regions of decreased solubility separated by a region of full solubility, which is denoted as region I. The first region of decreased solubility corresponds to DNA condensation and can be divided into

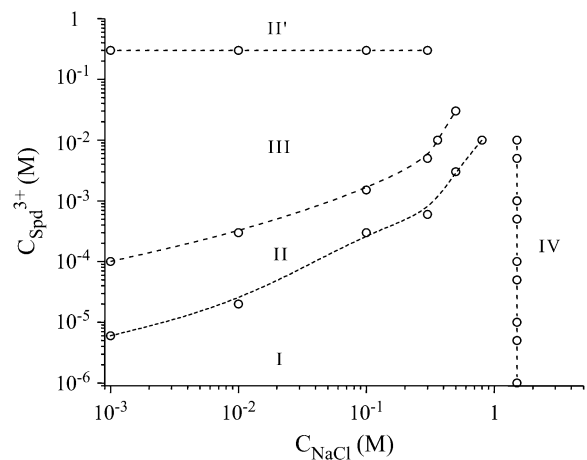


FIGURE 4 Plot of the concentrations  $C_1$ ,  $C_2$ ,  $C_3$ ,  $C_A$ ,  $C_B$ , and  $C_S$  in the plane of coordinates ( $[\text{NaCl}]$ ,  $[\text{Spd}^{3+}]$ ) in  $\text{D}_2\text{O}$ . Five distinct regions are observed. Regions I, II, III, and II' are delimited by dashed lines, which are guides for the eyes. Region I, the soluble phase; Regions II and II', regions where the solubility of DNA in the presence of  $\text{Spd}^{3+}$  varies; Region III, a region where solubility of DNA in the presence of  $\text{Spd}^{3+}$  is constant and minimal; and Region IV, a region above which the DNA is salted out by NaCl, separated from region I by a dashed vertical line at 1.5 M NaCl.

three subregions denoted II, III, and I'. The second region of decreased solubility corresponds to salting out and is denoted region IV. Regions I and IV are separated by a vertical line of fixed NaCl concentration. In other words, the concentration  $C_S$  is independent of the presence of  $\text{Spd}^{3+}$ . DNA condensation regions II, III, and I' are observed at lower NaCl concentrations (0.8 M and below). Region III corresponds to the plateau of minimal solubility, and in region II the solubility varies. This region of variable solubility corresponds to a narrow zone surrounding region III. In region I', the DNA is fully resolubilized. However, experiments described below show that this region indeed differs from region I. At high  $\text{Spd}^{3+}$  concentrations, we did not determine a boundary between regions I' and I, nor between regions I and IV. The general shape of regions III and II is triangular, with a rounded tip at high NaCl concentration. At lower spermidine concentrations, the boundaries between regions I and II and between II and III depend on the NaCl concentration, increasing with an increasing NaCl concentration between 1 mM and 200 mM. In contrast, at high spermidine concentrations, the boundaries between regions III and II and between regions II and I' are independent of the NaCl concentration, in the range 1–200 mM.

Fig. 4 shows the phase diagram observed in  $\text{D}_2\text{O}$ .

We again observe two regions of decreased DNA solubility separated by a region of full solubility. The general shape of the phase diagram obtained in  $\text{H}_2\text{O}$  is conserved: We can again define four regions, labeled I–IV, that have the same meanings as in the previous phase diagram, as well as a new region denoted II'. Because of the lower solubility of  $\text{Na}^+$  and  $\text{Spd}^{3+}$  in  $\text{D}_2\text{O}$ , we could not study the regions of simultaneous high concentrations of  $\text{Na}^+$  and  $\text{Spd}^{3+}$  (upper right corner of Fig. 4). As a result, the boundaries between the five regions are less well defined. In region I, the DNA is fully soluble. It is bounded at high NaCl concentrations by a vertical line at 1.5 M, up to a concentration of 10 mM of  $\text{Spd}^{3+}$ . At higher NaCl concentrations, region IV again corresponds to salting out. The concentration of salting out,  $C_S$ , is observed to be independent of the presence of spermidine. Region III also corresponds to the plateau of minimal solubility. In regions II and II', the solubility varies. In contrast to the previous phase diagram, we do not know if these two regions are connected, and thus we distinguish between the two. The shape of region III is still triangular. The boundary between regions I and II between 1 and 100 mM NaCl appears at much lower  $\text{Spd}^{3+}$  concentrations. The extension of region I is globally much smaller in  $\text{D}_2\text{O}$  than in  $\text{H}_2\text{O}$ , indicating a general decrease of DNA solubility, with the exception of the region defined by:  $0.25 \text{ M} \leq [\text{NaCl}] \leq 0.8 \text{ M}$  and  $10^{-3} \text{ M} \leq [\text{Spd}^{3+}] \leq 0.1 \text{ M}$ , where the opposite trend is observed. The decrease in DNA solubility in  $\text{D}_2\text{O}$  compared to  $\text{H}_2\text{O}$  results from a translation of the boundaries between regions I and II and regions II and III toward lower  $\text{Spd}^{3+}$  concentrations in the phase diagram obtained in  $\text{D}_2\text{O}$ . These two boundaries depend on the NaCl concentration, as in the

case of  $\text{H}_2\text{O}$ . The boundary between regions III and II' is independent of the NaCl concentration in the range 1–300 mM, as in the case of  $\text{H}_2\text{O}$ . In addition, this boundary is identical in  $\text{H}_2\text{O}$  and  $\text{D}_2\text{O}$  and therefore does not depend on the solvent.

### Solubility studies combining autoradiography and sedimentation

In these experiments, we determined by autoradiography the DNA concentration profiles in various regions of the phase diagram obtained for  $\text{H}_2\text{O}$ . In Figs. 5–7, the solid and shaded curves show the DNA concentration profiles obtained before and after centrifugation, respectively.

#### Salting out

Fig. 5 *a* shows the DNA concentration profile (expressed per unit length) obtained in the presence of 1 M NaCl (no added  $\text{Spd}^{3+}$ ), thus within region I (full solubility) of the phase diagram as determined for  $\text{H}_2\text{O}$  (Fig. 3). The solid and the shaded curves can be superimposed and have three parts: The central flat zone corresponds to the cylindrical section of the tube. Its relative flatness indicates that the DNA concentration is homogeneous. In the left part, the intensity decays over a length of  $\sim 2$  cm, starting at the air-water interface. This corresponds to  $\beta$ -particles emitted to air above the radioactive DNA in the aqueous solution. In the right of the graph, we observe a decrease in the intensity. This decrease starts at the beginning of the conical section, and finishes after the end of tube.

Fig. 5 *b* shows the profiles obtained in the presence of 4 M NaCl (again, in the absence of  $\text{Spd}^{3+}$ ), thus in the salting-out region IV of the phase diagram. Before centrifugation, there is a peak around the position of the air-water interface followed by a decreasing gradient of concentration. A peak is observed at  $\sim 70$  mm. After centrifugation, the concentration profile remains unchanged.

#### Solubility in the presence of $\text{Spd}^{3+}$ and NaCl

Fig. 6 shows the profiles obtained with increasing  $\text{Spd}^{3+}$  concentrations at a fixed NaCl concentration (10 mM):

At  $10^{-6}$  M  $\text{Spd}^{3+}$ , in region I of the phase diagram, the concentration profile is flat before centrifugation, indicating a homogeneous solution. After centrifugation, a weak peak at the air-water interface is visible, but the concentration profile remains essentially flat, as before.

At  $2.5 \times 10^{-4}$  M  $\text{Spd}^{3+}$ , in the middle of region II, there is a strong peak at the air-water interface, both before and after centrifugation. There is no evidence for a precipitate (the minimum visible at 60 mm in the intensity corresponds to a defect on the image plate). The intensity of the peak is clearly lowered by centrifugation, which implies the transfer of material; however, we do not see the appearance of a pellet at the bottom of the tube.

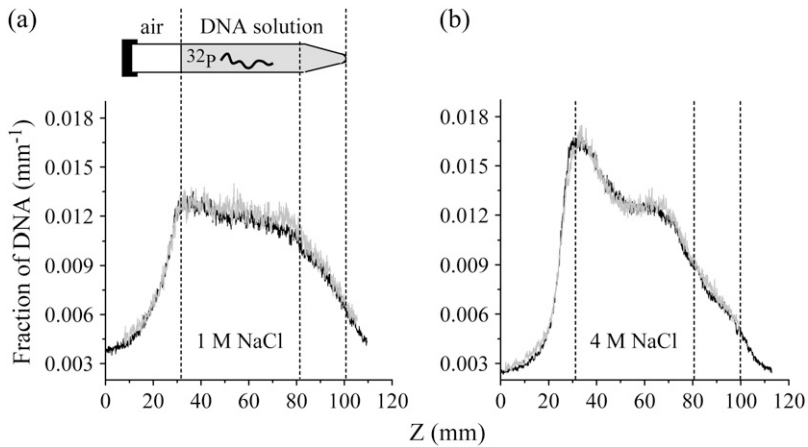


FIGURE 5 DNA concentration profile (per unit length) along the height of the tubes. (*Solid lines*) Concentration profiles before centrifugation. (*Shaded lines*) Concentration profiles after centrifugation. The dashed vertical lines indicate (*left to right*) the position of the air-water interface, the end of the cylindrical section of the tube, and the end of the conical section of the tube. (*a*) 1 M NaCl. A drawing of a Falcon tube is shown at the top of the figure. (*b*) 4 M NaCl.

At  $5 \times 10^{-2}$  M  $\text{Spd}^{3+}$ , in the middle of region III, before centrifugation, there is a maximum at the air-water interface, followed by a regularly decreasing gradient of concentration. After centrifugation, the peak has essentially disappeared and is replaced by a strong peak at the bottom of the tube, corresponding to a precipitated pellet.

At 1 M  $\text{Spd}^{3+}$ , in region I', the DNA is fully resolubilized according to the sedimentation studies described above. Before centrifugation, unexpectedly, we observe a clear maximum at the air-water interface, followed by a decreasing gradient of DNA concentration. After centrifugation, the DNA profile is flat, indicating a homogeneous distribution of the radio-labeled material in the tube, in agreement with the results of the sedimentation studies described above.

Fig. 7 shows the profiles obtained with increasing NaCl concentrations at a fixed  $\text{Spd}^{3+}$  concentration (10 mM). Without added NaCl (0 M NaCl), in the middle of region III, before centrifugation, there is a peak at the air-water interface,

followed by a decreasing gradient of concentration. After centrifugation, there are two peaks with equal intensities, at the air-water interface and at the bottom of the tube, indicating the presence of a pellet.

At 0.8 M NaCl, in region II, close to full resolubilization, there is a peak at the air-water interface, followed by a weakly decreasing gradient of DNA concentration. This profile is only weakly perturbed after centrifugation, with a small decrease of the peak at the air-water interface and a small transfer of material to the rest of the tube, and without a visible pellet.

At 1 M NaCl, the DNA is fully soluble according to the sedimentation studies described above. Unexpectedly, the profile before centrifugation reveals a peak at the air-water interface followed by a decreasing gradient of DNA concentration. After centrifugation, the DNA profile is flat, indicating a homogeneous distribution of DNA in the tube, in agreement with the result of the sedimentation studies described above.

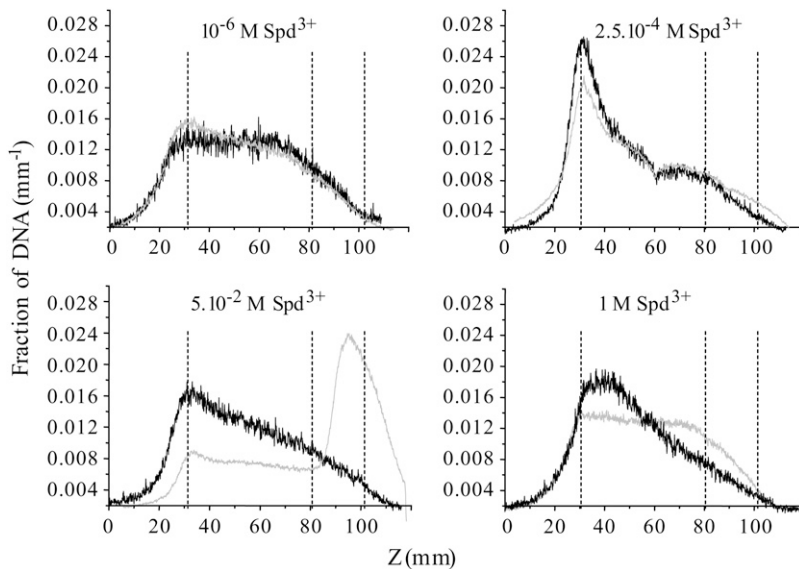


FIGURE 6 DNA concentration profiles along the height of the tubes at  $10^{-2}$  M NaCl for four  $\text{Spd}^{3+}$  concentrations. Lines are profiles of concentration before (*solid*) and after (*shaded*) centrifugation. The dashed vertical lines indicate (*left to right*) the position of the air-water interface, the end of the cylindrical section of the tube, and the end of the conical section of the tube.

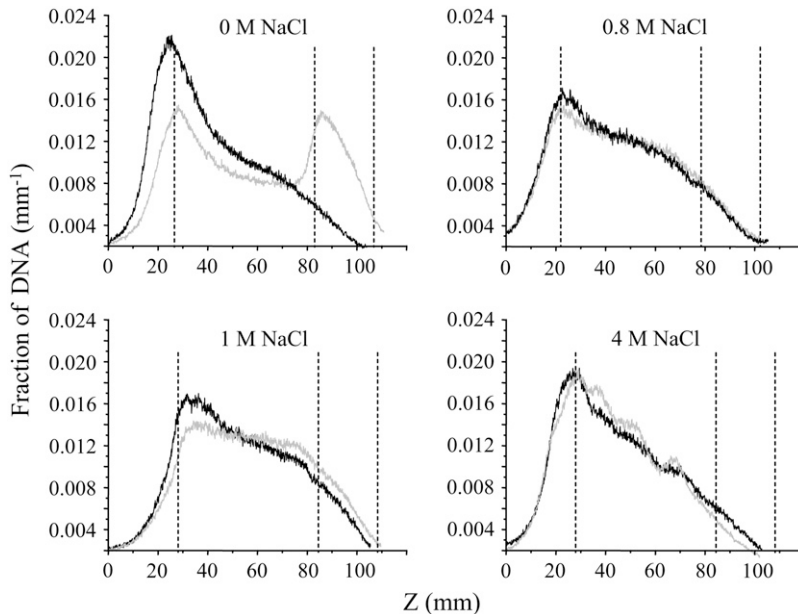


FIGURE 7 DNA concentration profiles along the height of the tubes at  $10^{-2}$  M  $\text{Spd}^{3+}$  for four NaCl concentrations. Lines represent concentration profiles before (*solid*) and after (*shaded*) centrifugation. The dashed vertical lines indicate (*left to right*) the position of the air-water interface, the end of the cylindrical section of the tube, and the end of the conical section of the tube.

At 4 M NaCl, in region IV, there is a strong peak at the air-water interface before centrifugation, which remains unchanged after centrifugation.

## DISCUSSION

### General shape of the phase diagrams describing the solubility of DNA

We studied the decrease of solubility of single-stranded DNA in the presence of monovalent (sodium) and multivalent (spermidine) cations, and obtained phase diagrams in  $\text{H}_2\text{O}$  and in  $\text{D}_2\text{O}$  (Figs. 3 and 4). We shall first compare these phase diagrams with those described in the literature, generally at much higher DNA concentrations.

At high DNA concentrations, NaCl and spermidine are known to promote two types of aggregation/precipitation: High concentrations of monovalent cations aggregate DNA and other polyelectrolytes by a phenomenon called salting out, which is also referred to as an H-type precipitation (high critical salt concentration) (24,28,33,34). In this type of precipitation, the critical salt concentration required to promote aggregation is basically independent of the concentration of DNA. The second type of aggregation is promoted by multivalent cations and is generally referred to as DNA condensation (5). In contrast to salting out with monovalent salts, the critical amount of multivalent cations required to promote aggregation is known to depend in a complex manner on the polyelectrolyte concentrations (25,27,35). However, at very low concentrations of single-stranded DNA, the critical multivalent concentration is independent of the single-stranded DNA concentration (up to  $10 \mu\text{g ml}^{-1}$ ) (26,27), and this corresponds to our experimental situation. Both salting out and condensation are studied here under conditions expected to be independent of

the single-stranded DNA concentration. This allows us to compare our phase diagrams with those obtained previously at somewhat higher but still low ( $<10 \mu\text{g ml}^{-1}$ ) DNA concentrations. In addition, we are able to compare directly the results obtained in the experiments using Eppendorf and Falcon tubes, even though the single-stranded DNA concentration differs by a factor of 3 in the two cases.

The phase diagrams reported here (Figs. 3 and 4) allow us to consider the two phenomena of salting out and condensation on the same graph. The phase diagrams obtained for both  $\text{H}_2\text{O}$  and  $\text{D}_2\text{O}$  define broadly two regions of phase separation in the plane of coordinates ( $[\text{NaCl}]$ ,  $[\text{Spd}^{3+}]$ ). The first region (IV) corresponds to the salting out regime, whereas the second (regions II and III in  $\text{H}_2\text{O}$ ; II, III, and II' in  $\text{D}_2\text{O}$ ) corresponds to the condensation regime requiring the presence of multivalent cations. The general shape of these phase diagrams is in accordance with the results obtained previously for single-, double-, and triple-stranded DNA, and other polyelectrolytes at low polymer concentrations (24–28,36). The triangular shape of the condensation regime in the presence of  $\text{Spd}^{3+}$  is well established. The independence of the salting-out concentration,  $C_s$ , on the concentration of  $\text{Spd}^{3+}$  (yielding the vertical lines in the phase diagrams) is expected, given the relative concentrations of the two salts in the system ( $>1$  M for NaCl and  $<0.1$  M for  $\text{Spd}^{3+}$ ).

### Decreased solubility of DNA in $\text{D}_2\text{O}$

A new result is the overall decreased solubility of  $\phi\text{X174}$  DNA in  $\text{D}_2\text{O}$  compared to  $\text{H}_2\text{O}$ . This decrease is characterized by two features: 1), Region I is globally shrunken in the  $\text{D}_2\text{O}$  phase diagram; and 2), DNA solubility in the presence of spermidine on the plateau of minimal solubility (region

III) is smaller for D<sub>2</sub>O ( $5 \pm 5\%$ ) than for H<sub>2</sub>O ( $20 \pm 10\%$ ). However, a closer look reveals a more complex situation:

1. The shrinking of region I is due to the greater efficiency of both spermidine and sodium chloride as phase-separating agents.
2. This greater efficiency for spermidine is only true at low concentrations: indeed, at high concentrations ( $>0.1$  M spermidine), identical amounts of spermidine are required to leave the plateau of minimal solubility in H<sub>2</sub>O and in D<sub>2</sub>O. In this case, neither the solvent nor NaCl concentration appear to play a role in this phenomenon, and redissolution depends solely on Spd<sup>3+</sup> concentration.
3. Last, there is a region in the plane of coordinates ([NaCl], [Spd<sup>3+</sup>]) ( $0.25 \text{ M} \leq [\text{NaCl}] \leq 0.8 \text{ M}$  and  $10^{-3} \text{ M} \leq [\text{Spd}^{3+}] \leq 0.1 \text{ M}$ ) where DNA is not soluble in H<sub>2</sub>O but is soluble in D<sub>2</sub>O.

The observation of a decreased solubility in D<sub>2</sub>O is well established for proteins (see, for instance, (37) and references therein). To our knowledge, it has not been reported for nucleic acids. This result could have been anticipated for the following reason: von Hippel and Schleich have observed that there is a general correlation between solubility and stability of biopolymers (34). Those compounds that stabilize the folded, helical form of biopolymers are also those that decrease their solubility. D<sub>2</sub>O has been shown to increase the melting temperature of double-stranded DNA (38), and therefore was expected to decrease the solubility of nucleic acids.

The origin of this decreased solubility of nucleic acids is complex. It is well known that simple salts (such as NaCl) are generally less soluble in D<sub>2</sub>O, and that the ionization constants of acids and bases are weaker in D<sub>2</sub>O. As a result, differences in charge state account partially for the decreased solubility of proteins in D<sub>2</sub>O (37). Here, a similar reasoning can be applied to the negative charges carried by the phosphate groups. The observed differences in solubility cannot result from electrostatic interactions alone, since D<sub>2</sub>O and H<sub>2</sub>O have very close dielectric constants. Therefore hydration, the other major force involved in the attraction between DNA molecules (30,31), must play a role both in salting out and in condensation. The overall decrease in the DNA solubility in D<sub>2</sub>O provides a direct evidence for a role of hydration in the two phenomena. The overall decrease in the DNA solubility in D<sub>2</sub>O provides a direct evidence for a role of hydration in the two phenomena.

### Significance of the phase diagrams: a role for adsorption

What is the significance of these phase diagrams? According to the literature, the phase-separation regions correspond to areas where a bulk aggregation occurs, leading to the formation of a sedimentation pellet after centrifugation: a bulk aggregation of nucleic acids has indeed been reported, but this does not rule out a concomitant adsorption at the air-water

interface. To investigate this issue, we performed studies combining autoradiography without or with centrifugation.

We discuss first the main features of our approach. We used <sup>32</sup>P to label DNA. This radioisotope emits high-energy  $\beta$ -particles, which allows us to work with very dilute solutions and to obtain DNA concentration profiles for the whole tube. At the same time, these particles have a penetration depth close to 1 cm in water, and this limits the spatial resolution of our experiments. DNA adsorbed at the water-phenol interface, for instance, produces a peak with an observed width of  $\sim 1$  cm in these conditions (13), and this is the typical spatial resolution of our system. This led to the use of long tubes (7 cm between the air-water interface and the bottom of the tube).

The observation of a flat concentration profile indicates the existence of a homogeneous DNA distribution in the tube, and this is observed in region I of the phase diagram (Figs. 5 a and 6, at  $10^{-6}$  M Spd<sup>3+</sup>). Outside of this region, and before centrifugation, we always observe two main phenomena. The first is the existence of a peak of DNA concentration at the air-water interface, and the second is the presence of a decreasing gradient of DNA concentration.

The presence of a peak at the air-water interface indicates an adsorption at this interface. According to the literature, the density of double-stranded DNA is greater than that of NaCl solutions between 0 and 4 M (39), and the density of single-stranded DNA exceeds that of double-stranded DNA (2). Thus, the presence of a peak of DNA located at the air-water interface cannot result from the flotation of the DNA chains in a solvent with a greater density.

The existence of the concentration gradient is not trivial. It is easy to estimate, with the Einstein relation, the mean distance,  $\sqrt{\langle r^2 \rangle}$ , that the DNA chains can explore by diffusion during the duration  $t$  of the experience (12–16 h), knowing their radius of gyration  $R_G$  ( $\sim 40$  nm at 0.1 M NaCl, (22), and  $<10$  times smaller in a compact, globular state):

$$\sqrt{\langle r^2 \rangle} = \sqrt{2t \frac{k_B T}{6\pi\eta R_G}}, \quad (2)$$

where  $k_B$  is the Boltzmann constant,  $T$  the room temperature, and  $\eta$  the viscosity of the solution (taken equal to that of water). One finds a distance of  $\sim 1$ –2 mm (for coil and globular states, respectively). Assuming that a diffusing chain becomes irreversibly adsorbed once it reaches the air-water interface, one would expect, after 12–16 h, the presence of an adsorption peak with a width of  $\sim 1$  cm (the spatial resolution of our technique), followed by a flat concentration profile. The existence of concentration gradients extending over several centimeters indicates that the system is not in equilibrium, and that diffusion alone does not account for our results. In addition, the experiment is more complex, since an ongoing aggregation is taking place in the solution. In view of these theoretical and experimental limitations, we shall not try to explain the detailed shapes of the concentration profiles (in

particular, the sharpness of the peaks observed at the air-water interface, the steepness of the concentration gradients, or the nature of secondary peaks, such as the peak observed at 70 mm in Fig. 5 b). Rather, we shall focus on the following phenomena: the presence or absence of a peak at the air-water interface, decrease of this peak after centrifugation, and the presence or absence of a pellet at the bottom of the tubes.

An analysis of the results obtained leads to the following findings:

1. In our very dilute solutions, the decrease in solubility is always associated with an adsorption at the air-water interface.
2. In the presence of spermidine, our centrifugation experiments lead to a simple understanding of the structure of the adsorbed material. It consists of aggregates that are large enough to migrate at low-speed centrifugation, either going back to the bulk of the solution, or forming a true pellet.
3. In the salting-out case, there is no evidence for a bulk aggregation after centrifugation. We have, apparently, an adsorption of either isolated DNA chains or of multimolecular aggregates that are too small to sediment. We know that at higher DNA concentrations, the same salt concentrations lead to the formation of a pellet after centrifugation. Therefore, we conclude that we are also in poor solvent conditions here. The individual single-stranded DNA chains are not expected to be in a random-coil state in the bulk of the solution, but to have a globular structure. The state of the chains at the air-water interface is unknown. They could remain as isolated globules or form small aggregates with other globules.
4. Finally, regions where the DNA is “soluble” just after centrifugation can, in reality, correspond to regions where an extensive adsorption takes place. This region, called  $I'$ , is observed at 10 mM NaCl and 1 M  $\text{Spd}^{3+}$  (Fig. 6), and 10 mM  $\text{Spd}^{3+}$  and 1 M NaCl (Fig. 7). In both cases, the transfer of the adsorbed DNA to the bulk of the solution after centrifugation implies the existence of DNA aggregates. Indeed, isolated chains are not expected to sediment efficiently under the mild centrifugation conditions employed. The aggregates are large enough to sediment, but they are too small to form a pellet. The presence of these aggregates strongly argues against a charge-reversal of the chains (a charge-reversed DNA is subject to electrostatic repulsion and will not aggregate); spermidine salts are not fully dissociated at high concentrations, and this provides a simpler explanation for their decreased efficiency as aggregating agents (40).

We conclude that in our experiments, the decrease in solubility is always associated with an adsorption. Furthermore, the adsorption is strictly coupled with the appearance of attractive interactions in the bulk of the solution, induced by monovalent salts at high concentrations or multivalent

salts at lower concentrations. These attractive interactions also lead to an aggregation, which may or may not lead to the sedimentation of the aggregates during centrifugation. Investigations of DNA salting out and condensation must therefore take into consideration this air-water adsorption, especially for very low DNA concentrations, where this effect may dominate.

### Comparison with the works of Frommer and Miller and Eickbush and Moudrianakis

The previous work of Frommer and Miller (20) showed that an adsorption of double-stranded and denatured DNA at the air-water interface can occur in the presence of monovalent salts at concentrations where the interaction between DNA monomers are repulsive. Similar results have been reported for double-stranded DNA in the presence of mono- and divalent salts by Eickbush and Moudrianakis (21). For denatured DNA, the adsorption is weak in the results of Frommer and Miller. In our case, we only observe adsorption under poor solvent conditions. The great difference between the DNA concentrations used by Frommer and Miller and those used in this study ( $\sim 1000$  times less), as well as the differences between  $\phi\text{X174}$  single-stranded DNA and denatured DNA, probably explain why we do not detect adsorption at lower sodium chloride concentrations. The experiments reported by Eickbush and Moudrianakis for double-stranded DNA in the presence of  $\text{Spd}^{3+}$  are qualitatively in agreement with our results obtained for single-stranded DNA. The only difference is that they observe a bulk precipitation in the absence of centrifugation, whereas we do not, but this can be due to the much lower DNA concentration used in our experiments ( $\sim 20$  times lower).

### Imperfect base pairing is not required for adsorption and aggregation

The single-stranded DNA of  $\phi\text{X174}$  can be partially double-stranded in the presence of salts, (41). For example, in solutions of moderate ionic strength (0.1–0.2 M NaCl), 36% of the nucleotides are in a B-type backbone conformation, due to imperfect base pairing (42). This observation raises two issues: 1), Is an intramolecular base pairing involved in the adsorption of single-stranded DNA? In other words, since the isolated chain is partially double-stranded, is the adsorption driven by the duplex regions of the chains? 2), Is intermolecular base pairing involved in the aggregation process?

Three arguments indicate that it is not the case for both issues. First, the phase diagrams obtained are not peculiar to single-stranded DNA. Similar phase diagrams are observed with double-stranded DNA, nucleosomes, and synthetic polyelectrolytes (27,28).

Second, a careful look to the phase diagrams shows that changes in solubility are observed with changes in salt concentration that weakly affect the stability of the partially

double-stranded portions of the DNA chain. For instance, the DNA is soluble up to 2.5 M NaCl in H<sub>2</sub>O. The melting temperature of native double-stranded DNA varies weakly above 2.5 M NaCl, being >90°C (43). The situation is similar for spermidine: in regions II and III of the phase diagrams, the concentrations of polyamines are such that the melting temperature is expected to be weakly affected by the addition of NaCl (44,45). We conclude that the changes in solubility observed are not correlated with changes in the secondary structure in the DNA chains.

Third, similar phase diagrams have been described for small single-stranded DNA chains (72, 99, and 118 bases) (26). In this work, the reversibility of the decrease in solubility in the presence of polyamines has been investigated. It was shown that the addition of NaCl is sufficient to reverse the solubility decrease. Now, this addition does not disrupt imperfect base pairing, but on the contrary further contributes to its stability. This result therefore shows that base pairing is not involved in the solubility decrease for these small chains.

### Mechanism of the adsorption and aggregation processes

A description of the mechanisms of the adsorption process, the aggregation process, and their relationship is delicate in view of the complexity of the system. The screening of electrostatic interactions is clearly involved, in the bulk and at the air-water interface. Beyond this factor, we shall discuss here the roles of van der Waals forces and quality of the solvent.

#### *A role for van der Waals interactions in adsorption and aggregation*

In our experiments, DNA adsorption is concomitant with a bulk aggregation: in the bulk of the solution, the DNA is in a dense state (condensed or salted out), and the formation of these dense states is known to be accompanied by a quasi-neutralization of the negative charges of the polyelectrolyte, as indicated for instance by electrophoretic mobility measurements (27,46) and calorimetry (32). We therefore must consider large, quasineutral particles of radius  $R$ . Katsura et al. (47) have shown that dense (globular) states of DNA can be trapped by optical tweezers. This finding implies that the refractive index of the dense states of DNA is higher than that of the surrounding aqueous buffer (48). Thus, there are three components in our system, the air, the buffer, and the DNA dense particles, with refractive indexes  $n_{\text{air}}$ ,  $n_{\text{buffer}}$ , and  $n_{\text{aggregate}}$ , respectively, and the indexes are ordered in the sequence:

$$n_{\text{aggregate}} > n_{\text{buffer}} > n_{\text{air}}. \quad (3)$$

Assuming that the shape of an aggregate is spherical, the van der Waals interaction potential between this macroscopic particle and the air/water interface is given by (49):

$$W(l) = -\frac{AR}{6l} \quad \text{for } l \ll R; \quad (4)$$

$$W(l) = -\frac{2AR^3}{9l^3} \quad \text{for } l \gg R, \quad (5)$$

where  $A$  is the Hamaker's constant,  $l$  is the distance between the interface and the aggregate, and  $R$  is the radius of the aggregate. Using the formula obtained by Hamaker (50) we can explicitly write the constant  $A$  as

$$A \approx \frac{3k_{\text{B}}T}{2} \left[ \frac{\sqrt{n_{\text{air}}} - \sqrt{n_{\text{buffer}}}}{\sqrt{n_{\text{air}}} + \sqrt{n_{\text{buffer}}}} \times \frac{\sqrt{n_{\text{aggregate}}} - \sqrt{n_{\text{buffer}}}}{\sqrt{n_{\text{aggregate}}} + \sqrt{n_{\text{buffer}}}} \right]. \quad (6)$$

According to Eqs. 3 and 6, the sign of  $A$  is explicitly negative. Thus, according to Eqs. 4 and 5, this leads to the appearance of attractive van der Waals forces trapping the DNA aggregate near the air-water interface (51). We note that these interactions cannot account for the large concentration gradients observed in Figs. 5–7.

The reasoning developed here also leads to a simple explanation of the late stages of the bulk aggregation process: The large, quasineutral particles with a refractive index  $n_{\text{aggregate}}$  will attract one another in a buffer of refractive index  $n_{\text{buffer}}$  through van der Waals interactions (51). We conclude that van der Waals interactions are involved both in the adsorption and in the late stages of the bulk aggregation of DNA.

#### *A role for the quality of the solvent*

In addition to the role of van der Waals interactions, it is also important to consider the local structure of the solvent near the interface, for a polymer adsorption process taking place in an extremely dilute system, and in a poor solvent. This has been considered from a theoretical point of view by Johner and Joanny (52) who predicted the existence of different regimes of adsorption, which may involve partial or complete wetting of the interface by the polymer, depending on the length and the concentration of the polymer and the strength of the interaction with the interface. At very low bulk concentrations the adsorbed chains could form a two-dimensional dilute polymer solution, which is either in a poor solvent, or in a good solvent. To our knowledge, these predictions have not been investigated experimentally.

In our experiments in the presence of spermidine, the adsorbed chains can be transferred to the bulk of the solution under mild centrifugation, and this indicates that the adsorbed chains always belong to large aggregates, excluding a good solvent scheme. Such a scheme cannot be ruled out in the salting-out case.

At low to moderate salt concentrations, one expects the existence of a local depletion region for the small ions (sodium chloride, spermidine) near the air-water interface, because of the charge image effect (53). The width of this region is  $\sim 10 \text{ \AA}$ . If the bulk of the solution is a poor solvent

for the single-stranded DNA chains, the region close to the interface could be a better solvent. This would induce a transfer of segments of the DNA chains from the bulk to this region. It would be a weak adsorption, which does not involve hydrophobic interactions, as those would have a visible effect on the surface tension, which is not observed by Frommer and Miller. Indeed, those authors showed that DNA adsorption does not alter the surface tension and surface potential. The situation in the presence of high concentrations of NaCl is even more delicate, since the salt concentration profile in this case is still debated (54). To summarize, we believe that the single-stranded DNA is only weakly adsorbed at the air-water interface. A similar analysis has been made in the case of polystyrene sulfonate in the presence of KCl (55), where it was shown that the adsorption layer is not well defined, suggesting that only a few monomers are actually anchored at the air-water interface. A bulk aggregation has also been observed in the same experimental conditions, but a rigorous investigation of the coupling between adsorption and aggregation was not considered.

### Implications

Our results have implications for the interpretation of phase diagrams of DNA and salts. We have seen that a decreased solubility cannot be simply equated with an aggregation. The field of DNA condensation, in particular, experiments using very dilute DNA solutions, must take into consideration these results. For instance, a monomolecular collapse of long double-stranded DNA chains has been observed in the DNA concentration range used (56,57). It is also the concentration range where DNA condensing agents have been shown to increase the rate of DNA renaturation or that of DNA cyclization (7,15,26). The role of an adsorption in these experiments should be investigated. Finally, processes leading to high local concentrations of nucleic acids are expected to be extremely relevant to prebiotic chemistry, in the perspective of an RNA world. Phase separation processes are among these and include aggregation and adsorption on solid surfaces such as clays, or liquid-liquid interfaces (see (13) and further references therein). The adsorption at the air-water interface is yet another process that should be taken into consideration. Single-stranded DNA, a single-stranded polynucleotide, has common features with RNA and the data obtained here are also of interest in this perspective.

### CONCLUSIONS

There is a strict correlation between adsorption and aggregation in these experiments. DNA adsorption involves attractive van der Waals forces, and these forces are also operating in the bulk aggregation process.

We thank Alan Braslau for constant support, numerous useful discussions, and careful reading of the manuscript. We also thank Theo Odijk and Eric

Raspaud and the referees and editor for their help in improving the manuscript.

This work was supported by an Action Concertée Incitative Physicochimie de la Matière Complexe of the Ministère de la Recherche et de la Technologie.

### REFERENCES

1. Felsenfeld, G., and H. T. Miles. 1967. Physical and chemical properties of nucleic acids. *Annu. Rev. Biochem.* 36:407–448.
2. Bloomfield, V. A., D. M. Crothers, and I. Tinoco, Jr. 1974. *Physical Chemistry of Nucleic Acids*. Harper and Row, New York.
3. Record, M. T., Jr., C. F. Anderson, and T. M. Lohman. 1978. Thermodynamic analysis of ion effects on the binding and conformational equilibria of proteins and nucleic acids: the roles of ion association or release, screening and ion effects on water activity. *Q. Rev. Biophys.* 11:103–178.
4. Cantor, C. R., and P. R. Schimmel. 1980. *Biophysical Chemistry. Part III. The Behavior of Biological Macromolecules*. W. H. Freeman, New York.
5. Bloomfield, V. A., D. M. Crothers, and I. Tinoco, Jr. 2000. *Nucleic Acids. Structure, Properties and Functions*. University Science Books, Herndon, VA.
6. Odijk, T. 1998. Osmotic compaction of supercoiled DNA into a bacterial nucleoid. *Biophys. Chem.* 73:23–29.
7. Sikorav, J.-L., and G. M. Church. 1991. Complementary recognition in condensed DNA: Accelerated DNA renaturation. *J. Mol. Biol.* 222: 1085–1108.
8. Pollack, G. H. 2003. The role of aqueous interfaces in the cell. *Adv. Colloid Interface Sci.* 103:173–196.
9. Kahn, M. E., and H. O. Smith. 1984. Transformation in hemophilus. A problem in membrane biology. *J. Membr. Biol.* 81:89–103.
10. White, J. H. C., N. R. Cozzarelli, and W. R. Bauer. 1988. Helical repeat and linking number of surface-wrapped DNA. *Science.* 241: 323–327.
11. Bates, A. D., and A. Maxwell. 1993. *DNA Topology*. Oxford University Press, Oxford, UK.
12. Alberts, B., A. Johnson, J. Lewis, M. Raff, K. Roberts, and P. Walter. 2002. *Molecular Biology of the Cell*. Garland, New York.
13. Goldar, A., and J.-L. Sikorav. 2004. DNA renaturation at the water-phenol interface. *Eur. Phys. J. E.* 14:211–239.
14. Chaperon, I., and J.-L. Sikorav. 1998. Renaturation of condensed DNA studied through a decoupling scheme. *Biopolymers.* 46:195–200.
15. Jary, D., and J.-L. Sikorav. 1999. Cyclization of globular DNA. Implications for DNA-DNA interactions in vivo. *Biochemistry.* 38: 3223–3227.
16. Rivetti, C., M. Guthold, and C. Bustamante. 1996. Scanning force microscopy of DNA deposited onto mica: equilibration versus kinetic trapping studied by statistical polymer chain analysis. *J. Mol. Biol.* 264:919–932.
17. Hansma, H. G. 2001. Surface biology of DNA by atomic force microscopy. *Annu. Rev. Phys. Chem.* 52:71–92.
18. Fang, Y., and J. H. Hoh. 1998. Early intermediates in spermidine-induced DNA condensation on the surface of mica. *J. Am. Chem. Soc.* 120:8903–8909.
19. Hansma, H. G., R. Golan, W. Hsieh, C. P. Lollo, P. Mullen-Ley, and D. Kwok. 1998. DNA condensation for gene therapy as monitored by atomic force microscopy. *Nucleic Acids Res.* 26:2481–2487.
20. Frommer, M. A., and I. R. Miller. 1968. Adsorption of DNA at the air-water interface. *J. Phys. Chem.* 72:2862–2866.
21. Eickbush, T. H., and E. N. Moudrianakis. 1977. Mechanism for entrapment of DNA at an air-water-interface. *Biophys. J.* 18:275–288.

22. Sinsheimer, R. L. 1959. Single-stranded deoxyribonucleic acid from bacteriophage  $\phi$ X174. *J. Mol. Biol.* 1:43–53.
23. Eisenberg, H., and G. Felsenfeld. 1967. Studies of temperature-dependent conformation and phase separation of polyriboadenylic acid solutions at neutral pH. *J. Mol. Biol.* 30:17–37.
24. Pelta, J., F. Livolant, and J.-L. Sikorav. 1996. DNA aggregation induced by polyamines and cobalthexamine. *J. Biol. Chem.* 271:5656–5662.
25. Raspaud, E., M. O. de la Cruz, J.-L. Sikorav, and F. Livolant. 1998. Precipitation of DNA by polyamines: a polyelectrolyte behavior. *Biophys. J.* 74:381–393.
26. Chaperon, I. 1999. A study of DNA condensation and DNA renaturation. Université Paris-Sud, Paris.
27. Raspaud, E., I. Chaperon, A. Leforestier, and F. Livolant. 1999. Spermine-induced aggregation of DNA, nucleosome, and chromatin. *Biophys. J.* 77:1547–1555.
28. de la Cruz, M. O., L. Belloni, M. Delsanti, J. P. Dalbiez, O. Spalla, and M. Drifford. 1995. Precipitation of highly-charged polyelectrolyte solutions in the presence of multivalent salts. *J. Chem. Phys.* 103: 5781–5791.
29. Edsall, J. T., and J. Wyman. 1958. *Biophysical Chemistry*. Academic Press, New York.
30. Rau, D. C., and V. A. Parsegian. 1992. Direct measurement of the intermolecular forces between counterions-condensed DNA double helices - evidence for long-range attractive hydration forces. *Biophys. J.* 61:246–259.
31. Parsegian, V. A., R. P. Rand, and D. C. Rau. 1995. Macromolecules and water: probing with osmotic stress. *Methods Enzymol.* 259:43–94.
32. Matulis, D., I. Rouzina, and V. A. Bloomfield. 2000. Thermodynamics of DNA binding and condensation: isothermal titration calorimetry and electrostatic mechanism. *J. Mol. Biol.* 296:1053–1063.
33. Ikegami, A., and N. Imai. 1962. Precipitation of polyelectrolytes by salts. *J. Polym. Sci. [BJ]* 56:133–152.
34. von Hippel, P. H., and T. Schleich. 1969. The effects of neutral salts on the structure and conformational stability of macromolecules in solution. In *Structure and Stability of Biological Macromolecules*. S. N. Timasheff and G. Fasman, editors. Marcel Dekker, New York. 417–574.
35. Burak, Y., G. Ariel, and D. Andelman. 2003. Onset of DNA aggregation in presence of monovalent and multivalent counterions. *Biophys. J.* 85:2100–2110.
36. Saminathan, M., T. Antony, A. Shirahata, L. H. Sigal, T. Thomas, and T. J. Thomas. 1999. Ionic and structural specificity effects of natural and synthetic polyamines on the aggregation and resolubilization of single-, double-, and triple-stranded DNA. *Biochemistry.* 38:3821–3830.
37. Larsson, U. 1988. Polymerization and gelation of fibrinogen in D<sub>2</sub>O. *Eur. J. Biochem.* 174:139–144.
38. Izzo, V. S., S. Fornili, and L. Cordone. 1975. Thermal denaturation of *B. subtilis* DNA in H<sub>2</sub>O and D<sub>2</sub>O observed by electron microscopy. *Nucleic Acids Res.* 2:1805–1810.
39. Cohen, G., and H. Eisenberg. 1968. Deoxyribonucleate solutions: sedimentation in a density gradient, partial specific volumes, density and refractive index increments, and preferential interactions. *Biopolymers.* 6:1077–1100.
40. Yang, J., and D. C. Rau. 2005. Incomplete ion dissociation underlies the weakened attraction between DNA helices at high spermidine concentrations. *Biophys. J.* 89:1932–1940.
41. Blakesley, R. W., J. B. Dodgson, I. F. Nes, and R. D. Wells. 1977. Duplex regions in “single-stranded”  $\phi$ X174 DNA are cleaved by a restriction endonuclease from *Haemophilus aegyptius*. *J. Biol. Chem.* 252:7300–7306.
42. Benevides, J. M., P. L. Stow, L. Ilag, N. L. Incardona, and G. J. Thomas, Jr. 1991. Differences in secondary structure between packaged and unpackaged single-stranded DNA of bacteriophage  $\phi$ X174 determined by Raman spectroscopy: a model for  $\phi$ X174 DNA packaging. *Biochemistry.* 3:195–208.
43. Schildkraut, C. 1965. Dependence of melting temperature of DNA on salt concentration. *Biopolymers.* 3:195–208.
44. Tabor, H. 1962. Protective effect of spermine and other polyamines against heat denaturation of deoxyribonucleic acid. *Biochemistry.* 1: 496–501.
45. Thomas, T. J., and V. A. Bloomfield. 1984. Ionic and structural effects on the thermal helix coil transition of DNA complexed with natural and synthetic polyamines. *Biopolymers.* 23:1295–1306.
46. Yamasaki, Y., Y. Teramoto, and K. Yoshikawa. 2001. Disappearance of the negative charge in giant DNA with a folding transition. *Biophys. J.* 80:2823–2832.
47. Katsura, S., K. Hirano, Y. Matsuzawa, K. Yoshikawa, and A. Mizuno. 1998. Direct laser trapping of single DNA molecules in the globular state. *Nucleic Acids Res.* 26:4943–4945.
48. Ashkin, A. 1970. Acceleration and trapping of particles by radiation pressure. *Phys. Rev. Lett.* 24:156–159.
49. Israelachvili, J. N. 1974. Van der Waals forces in biological-systems. *Q. Rev. Biophys.* 6:341–387.
50. Hamaker, H. C. 1937. The London-van der Waals attraction between spherical particles. *Physica.* 4:1058–1172.
51. Israelachvili, J. N. 1992. *Intermolecular and Surface Forces*. Academic Press, London.
52. Johner, A., and J. F. Joanny. 1991. Polymer adsorption in a poor solvent. *J. Phys. II.* 1:181–194.
53. Onsager, L., and T. N. Samaras. 1934. The surface tension of Debye-Hückel electrolytes. *J. Chem. Phys.* 2:528–536.
54. Garrett, B. C. 2004. Ions at the air/water interface. *Science.* 303:1146–1147.
55. Yim, H., M. S. Kent, A. Matheson, M. J. Stevens, R. Ivkov, S. Satija, J. Majewski, and G. S. Smith. 2002. Adsorption of sodium poly(styrenesulfonate) to the air surface of water by neutron and X-ray reflectivity and surface tension measurements: polymer concentration dependence. *Macromolecules.* 35:9737–9747.
56. Post, C. B., and B. H. Zimm. 1982. Light-scattering study of DNA condensation - competition between collapse and aggregation. *Biopolymers.* 21:2139–2160.
57. Widom, J., and R. L. Baldwin. 1983. Monomolecular condensation of  $\lambda$ -DNA induced by cobalt hexamine. *Biopolymers.* 22:1595–1620.